Lone Pair Functionality in Divalent Lead Compounds

Liat Shimoni-Livny,[†] Jenny P. Glusker,*[,†] and Charles W. Bock[†,‡]

The Institute for Cancer Research, Fox Chase Cancer Center, Philadelphia, Pennsylvania 19111, and
The Philadelphia College of Textiles and Science, Philadelphia, Pennsylvania 19144

Received July 24, 1997

The role of the lone pair of electrons of Pb(II) in determining the coordination geometry is analyzed from crystallographic studies and ab initio molecular orbital optimizations. Of particular interest are factors that contribute to the disposition of ligands around the lead with geometries that are (1) *holodirected*, in which the bonds to ligand atoms are distributed throughout the surface of an encompassing globe, and (2) *hemidirected*, in which the bonds to ligand atoms are directed throughout only part of an encompassing globe, i.e., there is an identifiable void in the distribution of bonds to the ligands. The preferred coordination numbers for lead were found to be 4 for Pb(IV) and 4 and 6 for Pb(II). *All* Pb(IV) structures in the CSD have a holodirected coordination geometry. Pb(II) compounds are hemidirected for low coordination numbers (2−5) and holodirected for high coordination numbers (9, 10), but for intermediate coordination numbers (6−8), examples of either type of stereochemistry are found. Ab initio molecular orbital studies of gas-phase Pb(II) complexes show that a hemidirected geometry is favored if the ligand coordination number is low, the ligands are hard, and there are attractive interactions between the ligands. In such complexes, the lone pair orbital has p character and fewer electrons are transferred from the ligands to the bonding orbitals of Pb(II), resulting in bonds that are more ionic. A holodirected geometry is favored when the coordination number is high and the ligands are soft and bulky or show strong interligand repulsion. The lone pair orbital has little or no p character when the geometry is holodirected, and the bonds are more covalent than in the hemidirected structures. The energy cost of converting a hemidirected to a constrained holodirected structure is of the order 8−12 kcal/mol in the absence of strong interligand interactions.

Introduction

Lead is an environmental pollutant with severe toxic effects. It has had important industrial uses in paints and in the construction of storage batteries. The mining of its ores for these purposes has led to significant atmospheric contamination. Poisoning by divalent lead, Pb(II), occurs as children nibble lead-containing paint or people drink from improperly lead-glazed utensils.[1] In its tetravalent state, Pb(IV), it was also used in gasoline because of the octane-improving (antiknock) characteristics of tetraethyllead which enabled manufacturers to use higher compression on the cylinders, thereby obtaining a higher efficiency.[2] Tetraethyllead, however, also caused significant pollution and continues to do so in countries that still permit its use. Treatment involves various chelating agents, but these are usually nonspecific and relatively toxic.[3]

The interaction of divalent lead with biological materials has been studied extensively. It appears that in this oxidation state lead binds preferentially to thiol and phosphate groups in nucleic acids, proteins, and cell membranes.[4−6] Polarographic and circular dichroism studies have indicated that Pb(II) has an overall stabilizing effect when it interacts with double-helical DNA.[7] By contrast, interactions of Pb(II) with RNA under biological conditions result in hydrolysis of the nucleic acid (with strand breakage), as in the case of yeast phenylalanine *t*RNA,[8,9] in which cleavage by millimolar concentrations of Pb(II) occurs mainly in the D-loop.[10−13] Pb(II) depolymerizes RNA faster than any other metal ion,[14] and, because RNA but not DNA is degraded in this way, the 2′-hydroxyl group is apparently involved in the reaction; it is presumed that a cyclic phosphate intermediate is formed when the 2′-hydroxyl group attacks the phosphorus atom. As a result, the phosphodiester P−O bond is broken.[15]

Pb(II) inhibits the synthesis of hemoglobin, causing anemia. One site of action is the enzyme porphobilinogen synthase (PBGS), a Zn^{II}-metalloenzyme involved in heme biosynthesis.[16−24]

---

* Corresponding author. Tel.: (215) 728 2220. FAX: (215) 728 2863. Internet: jp_glusker@fccc.edu.

[†] Fox Chase Cancer Center.

[‡] The Philadelphia College of Textiles and Science.

(1) Chisholm, J. J. *Sci. Am.* **1971**, *224*(2), 15−23.
(2) Midgley, T., Jr.; Boyd, T. A. *J. Ind. Eng. Chem.* **1922**, *14*, 589−593.
(3) Ratcliffe, J. M. *Lead in Man and Environment*; John Wiley & Sons: New York, 1981.
(4) Sigel, H.; Fischer, B. E.; Farkas, E. *Inorg. Chem.* **1983**, *22*, 925−934.
(5) Tajimir-Riahi, H. A.; Langlais, M.; Savoie, R. *Nucleic Acids Res.* **1988**, *16*, 751−762.
(6) Abu-Dari, K.; Hahn, F. E.; Raymond, K. N. *J. Am. Chem. Soc.* **1990**, *112*, 1519−1524.
(7) Gasiorowski, K.; Swiatek, J.; Kozlowski, H. *Inorg. Chim. Acta* **1985**, *106*, L1−L5.
(8) Dimroth, K.; Jaenicke, L.; Heinzel, D. *Ann. Chem.* **1950**, *566*, 206−210.
(9) Ciesiolka, J.; Wrzesinski, J.; Gornicki, P.; Podkowinski, J.; Krzyzosiak, W. *Eur. J. Biochem.* **1989**, *186*, 71−77.
(10) Werner, C.; Krebs, B.; Keith, G.; Dirheimer, G. *Biochim. Biophys. Acta* **1976**, *432*, 161−175.
(11) Marciniec, T.; Ciesiolka, J.; Wrzesinski, J.; Krzyzosiak, W. *FEBS Lett.* **1989**, *243*, 293−298.
(12) Otzen, D. E.; Barciszewski, J.; Clark, B. F. C. *Biochimie* **1994**, *76*, 15−21.
(13) Brown, R. S.; Dewan, J. C.; Klug, A. *Biochemistry* **1985**, *24*, 4785−4801.
(14) Farkas, W. R. *Biochim. Biophys. Acta* **1968**, *155*, 401−409.
(15) Pan, T.; Uhlenbeck, O. C. *Nature (London)* **1992**, *358*, 560−563.
(16) Jaffe, E. K.; Volin, M.; Mayers, C. B. *Biochemistry* **1994**, *33*, 11554−11562.

S0020-1669(97)00909-9 CCC: $15.00

Unlike most Zn^{II}-metalloenzymes, PBGS is sensitive to and inhibited by micromolar concentrations of Pb(II), and this inhibition is believed to contribute to the devastating toxicity of lead in children.[1,25-28] We are currently involved in structural studies of the enzyme PBGS and the various modes of binding and inhibition of this enzyme by lead.[29] We have also studied the crystal structure of D-xylose isomerase,[30] for which Pb-binding data are also available.[31] Another enzyme inhibited by lead is ferrochelatase, the enzyme that catalyzes the introduction of iron into the heme precursor.[1]

Divalent lead, with its electronic configuration $[Xe]4f^{14}5d^{10}6s^2$, is one of the post-transition metal elements that exhibits the so-called "inert-pair effect".[32-37] This term refers to the resistance of the pair of outer electrons on Pb(II) to removal or to participation in covalent bond formation or hydrogen bonding. It has been explained as a relativistic effect causing the 6s orbital to contract, thereby increasing the energy required to remove or interact with the 6s lone pair of electrons. On the other hand, the d and f orbitals are destabilized because they expand radially as a result of screening from nuclear attraction by the s and p electrons. The result is a stable, relatively inert outer lone pair of electrons.

This lone pair of electrons can cause a nonspherical charge distribution around the Pb(II) cation, that is, the disposition of ligands around the cation results in an identifiable void.[32] This gap in the coordination sphere has been considered evidence of a "stereochemically active lone pair of electrons" which probably takes up more space on a specific region of the surface of the coordination sphere than does a single bond.[38,39] It is becoming increasingly clear, however, that it is not necessarily true that one of the effects of the lone pair of electrons in Pb(II) compounds is to cause a void in the coordination geometry; in fact this geometry can take various forms.[40] For example, in an X-ray crystallographic and ^{207}Pb NMR study, one poly(pyrazolyl)borate complex of Pb(II) with very bulky ligands was shown to have a completely symmetrical arrangement of ligands, implying no stereochemical activity of the lone pair of electrons. Another similar complex, however, containing less bulky ligands, clearly showed a void in the distribution of ligands, implying a stereochemically active lone pair.[27]

In the design of drugs to counteract the effects of lead poisoning, it is necessary to establish the preferred ligands of lead and their stereochemistry and to compare these with the requirements of other essential metal ions such as zinc. From such information chelating agents can be designed to remove lead compounds (but not other cations) after ingestion in the human body.[3] In this article we describe various binding modes of lead in its divalent and tetravalent oxidation states. The methods used include an analysis of high-resolution, high-precision crystal structures, and ab initio molecular orbital optimizations of a variety of gas-phase lead complexes. The aim is to identify those conditions that influence whether the lone pair is stereochemically active or not and to analyze the conditions in terms of the preferred ligands and coordination numbers of the lead.

Methods

(a) Structural Studies. The binding preferences of lead were examined by a search of the Cambridge Structural Database (CSD)[41] (latest release, 1996) for compounds containing the element lead (Pb) in any of it oxidation states. The CSD input files, containing query information, were stored in instruction files (named *.que, where * is the name given to the study). The CSD program QUEST was used to search the database file for structures that matched the input requirements and to write the coordinates of these crystal structures onto a data file (*.dat). The CSD program GSTAT[41] was then run on this coordinate data file using the instruction file *.geo as input. The maximum effective sum of the van der Waals radii was set, for this study, at 3.5 Å so that the geometry of the intermolecular interactions around the lead ion could be found. All crystal structures reported here were illustrated on a computer graphics system by use of the program ICRVIEW which also provides any requested interatomic distances.[42] This enabled us to double-check the coordination geometry around the lead, particularly whether there was a void in the arrangement of ligands, and the interatomic distances involved.

The lead-containing compounds found in the CSD were separated according to their oxidation states and coordination numbers. The oxidation state of lead, i.e., II or IV, was determined from the reported chemical formula and/or from the title of the published article. If a crystal structure included more than one lead ion, with a different coordination number, separate entries were used for each lead ion. Complexes in which the lead ion is mainly liganded to other metals, e.g. Mo, Fe, etc., or liganded to a boron hydride ring were excluded from this analysis because their biological relevance was limited. Structures with high crystallographic *R* values or identified disorder were also eliminated in order to include only precise crystal structure determinations.

To check for any disorder in the lead atom position, which could affect our interpretation of the ligand stereochemistry in any given crystal structure, we examined the reported atomic displacement parameters of each lead atom to ensure that they were lower than values for the surrounding liganding atoms. These parameters express the amount of atomic vibration or disorder. Displacement parameters were generally lower for the lead than for surrounding atoms, indicating an ordered position for this atom; some exceptions were found in which

---

(17) Jaffe, E. K. *Comments Inorg. Chem.* **1993**, *15*, 67−92.
(18) Mitchell, L. W.; Jaffe, E. K. *Arch. Biochem. Biophys.* **1993**, *300*, 169−177.
(19) Jaffe, E. K.; Abrams, W. R.; Kaempfen, H. X.; Harris, K. A., Jr. *Biochemistry* **1992**, *31*, 2113-2123.
(20) Jaffe, E. K.; Markham, G. D.; Rajagopalan, J. S. *Biochemistry* **1990**, *29*, 8345−8350.
(21) Dent, A. J.; Beyersmann, D.; Block, C.; Hasnain, S. S. *Biochemistry* **1990**, *29*, 7822−7828.
(22) Jaffe, E. K.; Hannes, D. *J. Biol. Chem.* **1986**, *261*, 9348−9353.
(23) Jaffe, E. K.; Markham, G. D. *Biochemistry* **1987**, *26*, 4258−4264.
(24) Jaffe, E. K.; Markham, G. D. *Biochemistry* **1988**, *27*, 4475−4481.
(25) Needleman, H. L.; Gatsonis, H. L. *J. Am. Med. Assoc.* **1990**, *263*, 673−678.
(26) Harrison, R. M.; Laxer, D. P. H. *Lead Pollution*; Chapman and Hall: London, 1981.
(27) Reger, D. L.; Huff, M. F.; Reingold, A. L.; Haggerty, B. S. *J. Am. Chem. Soc.* **1992**, *114*, 579−584.
(28) Wang, S.; Mitzi, D. B.; Feild, C. A.; Guloy, A. *J. Am. Chem. Soc.* **1995**, *117*, 5297−5302.
(29) Carrell, H. L.; Glusker, J. P.; Shimoni, L.; Keefe, L. J.; Afshar, C.; Volin, M.; Jaffe, E. K. *Acta Crystallogr.* **1996**, *D*52, 419−421.
(30) Carrell, H. L.; Glusker, J. P.; Burger, V.; Manfre, F.; Tritsch, D.; Biellmann, J.-F. *Proc. Natl. Acad. Sci. U.S.A.* **1989**, *86*, 4440−4444.
(31) Sudfeldt, C.; Schäffer, A.; Kägi, J. H. R.; Bogumil, R.; Schulz, H.-P.; Wulff, S.; Witzel, H. *Eur. J. Biochem.* **1990**, *193*, 863−871.
(32) Sidgwick, N. V.; Powell, H. M. *Proc. R. Soc. (London)* **1940**, *A176*, 153.
(33) McKeney, D. R. *J. Chem. Educ.* **1983**, *60*, 112−116.
(34) Banna, M. S. *J. Chem. Educ.* **1985**, *62*, 197−198.
(35) Pitzer, K. S. *Acc. Chem. Res.* **1979**, *12*, 271−276.
(36) Pyykkö, P.; Desclaux, J.-P. *Acc. Chem. Res.* **1979**, *12*, 276−281.
(37) Pyykkö, P. *Chem. Rev.* **1988**, *88*, 563−594.
(38) Gillespie, R. J.; Nyholm, R. S. *Q. Rev. London* **1957**, *11*, 339−380.
(39) Gillespie, R. J.; Hargittai, I. *The VSEPR Model of Molecular Geometry*; Allyn and Bacon: Boston, MA, 1991. In the notation in this book $Pb^{II}\cdot 4H_2O$ would be designated $Pb^{II}X_4E$.
(40) Ng, S.-W.; Zuckerman, J. J. *Adv. Inorg. Chem. Radiochem.* **1985**, *29*, 297−319.
(41) Allen, F. H.; Bellard, S.; Brice, M. D.; Cartwright, B. A.; Doubleday: A.; Higgs, H.; Hummelink, T.; Hummelink-Peters, B. G.; Kennard, O.; Motherwell, W. D. S.; Rodgers, J. R.; Watson, D. G. *Acta Crystallogr.* **1979**, *B35*, 2331−2339.
(42) Erlebacher, J.; Carrell, H. L. *ICRVIEW, Program from the Institute for Cancer Research*; ICR: Philadelphia, PA.

the lead displacement parameters were much higher, suggesting a disordered lead position, and these entries were eliminated from the search. A list of compounds found in the CSD search and their bibliography and examples of *.que and *.geo files are given in Tables 1S−3S of the Supporting Information, respectively.

(b) Molecular Orbital Studies. *Ab initio* molecular orbital optimizations (with relativistic corrections, as described below) were performed on a variety of lead (Pb) complexes using second-order Møller−Plesset (MP2)[43] perturbation theory with the GAUSSIAN 94 series of programs[44] on the Cray YMP at the National Cancer Institute, Frederick, MD and on a DEC alpha 3000/600 workstation. The LANL2DZ basis set was used throughout, augmented by additional *d* functions on all the heavy atoms.[45] The LANL2DZ basis set uses the Dunning/Huzinaga full double-ζ (D95) basis set on atoms in the first row and the Los Alamos effective core potential plus DZ on Na to Bi.[46−49] This computational method incorporates the major relativistic effects (that is, Darwin and mass−velocity terms) by fitting the atomic pseudopotential parameters to relativistic all-electron Hartree−Fock (HF) atomic wave functions.[46−48] Molecular spin−orbit coupling is expected to be small for closed-shell species near their ground state and has not been considered in this study.[50−53]

Unless otherwise noted, optimizations were carried out with no symmetry constraints to avoid obtaining transition states, and, in many cases, the OPT=TIGHT option in GAUSSIAN 94 was used to tighten the cutoffs on the residual forces and displacements used as criteria for convergence.[44] Harmonic frequencies, calculated numerically from finite differences of the analytical first derivatives, and energies (analytical second derivatives are not available for this computational level) were obtained for some of the structures to confirm that they are local minima (not transition states) on the various potential energy surfaces.[54] The wave functions of the lead complexes were analyzed by natural bond orbital analyses, involving natural atomic orbital (NAO) populations and natural bond orbitals (NBO).[55,56] The Reed/Weinhold NAO/NBO analysis package is part of GAUSSIAN 94.[44]

Results

The surroundings of lead in crystal structures were inspected by use of the computer graphics program ICRVIEW;[42] a total of 329 unique entries of lead-containing crystal structures were selected from the CSD and used in our analysis. When there was more than one determination of a particular crystal structure, those entries with the higher *R* values were eliminated from our search. In addition, some lead-containing structures (48 in all) were excluded for reasons described in the Methods section. The coordination geometry of lead was examined in these 329 experimentally determined structures and compared with the results of ab initio molecular orbital calculations on a variety of gas-phase lead complexes; for the latter only coordination number 4 was investigated.

Scheme 1. (A) Holodirected and (B) Hemidirected Coordination

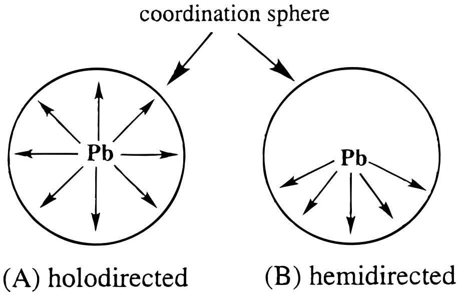

(a) Holodirected or Hemidirected Lead Coordination. The experimental coordination geometry around lead, reveals two distinct structural categories, shown as A and B in Scheme 1: (A) *holodirected*, in which the bonds to ligand atoms are directed throughout the surface of an encompassing globe, and (B) *hemidirected*, in which the bonds to ligand atoms are directed throughout only part of the globe, that is, there is an identifiable void (or gap) in the distribution of bonds to the ligands. Linear and planar structures are considered to be holodirected for coordination numbers 2 and 3, respectively. The classification of the structures in the CSD as holodirected or hemidirected was rarely ambiguous, although the "size" of the void varies considerably, particularly with the coordination number.[57] Examples of both coordination geometries are shown in Figure 1.[58−65]

All Pb(IV) compounds in the CSD show a holodirected coordination geometry (see Scheme 1A). For example, the geometry for coordination number 4 is that of a tetrahedron with the Pb(IV) at its center, as expected because Pb(IV) has no lone pair of electrons. Calculations by Kaupp and von Schleyer have shown, however, that there are significant deviations from ideal tetrahedral angles in the compounds $(CH_3)_nPb^{IV}X_{4-n}$ [X = F, Cl; n = 1−3] due to inductive substituent effects.[50]

---

(43) Møller, C.; Plesset, M. S. *Phys. Rev.* **1934**, *46*, 618−622.

(44) Frisch, M. J.; Trucks, G. W.; Schlegel, H. B.; Gill, P. M. W.; Johnson, B. G.; Robb, M. A.; Cheeseman, J. R.; Keith, T. A.; Peterson, G. A.; Montgomery, J. A.; Raghavachari, K.; Al-Laham, M. A.; Zakrzewski, V. G.; Ortiz, J. V.; Foresman, J. B.; Cioslowski, J.; Stefanov, B. B.; Nanayakkara, A.; Challacombe, M.; Peng, C. Y.; Ayala, P. Y.; Chen, W.; Wong, M. W.; Andres, J. L.; Replogle, E. S.; Gomperts, R.; Martin, R. L.; Fox, J. S.; Binkley, J. S.; Defrees, D. J.; Baker, J.; Stewart, J. P.; Head-Gordon, M.; Gonzales, C.; Pople, J. A. *GAUSSIAN 94*, Revision A.1; Gaussian, Inc.: Pittsburgh, PA, 1995.

(45) Huzinaga, S.; Andzelm, J.; Klobukowski, M.; Radzio-Andzelm, E.; Sakai, K.; Takewaki, H. *Gaussian Basis Sets for Molecular Calculations*; Elsevier: New York, 1984.

(46) Hay, P. J.; Wadt, W. R. *J. Chem. Phys.* **1985**, *82*, 270−283.

(47) Wadt, W. R.; Hay, P. J. *J. Chem. Phys.* **1985**, *82*, 284−298.

(48) Hay, P. J.; Wadt, W. R. *J. Chem. Phys.* **1985**, *82*, 299−310.

(49) Dunning, T. H., Jr.; Hay, P. J. *Modern Theoretical Chemistry*; Schaeffer, H. F., III, Ed.; Plenum: New York, 1976; pp 1−28.

(50) (a) Kaupp, M.; Schleyer, P. v. R. *J. Am. Chem. Soc.* **1993**, *115*, 1061−1073. (b) They observed that the presence of electronegative substituents decreases the transfer of electrons to the lead so that the valence density remaining for covalent bonding is mainly s in character, making efficient sp hybridization difficult, and resulting in significant deviations from idealized tetrahedral angles and weaker covalent bonds.

(51) Schwerdtfeger, P. *Phys. Scr.* **1987**, *36*, 453−459.

(52) Pitzer, K. S. *Int. J. Quantum Chem.* **1984**, *25*, 131−148.

(53) Schwerdtfeger, P.; Boyd, P. D. W.; Bowmaker, G. A.; Mack, H. G.; Oberhammer, H. J. *J. Am. Chem. Soc.* **1989**, *111*, 15−23.

(54) Pople, J. A.; Binkley, J. S.; Seeger, R. *Int. J. Quantum Chem.* **1976**, *10S*, 1−19.

(55) (a) Reed, A. E.; Curtiss L. A.; Weinhold, F. *Chem. Rev.* **1988**, *88*, 899−926. (b) Weinhold, F.; Carpenter, J. E. In *The Structure of Small Molecules and Ions*; Naaman R., Vager Z., Eds.; Plenum: New York, 1988; pp 227−236.

(56) Glendening, E. D.; Reed, A. E.; Carpenter, J. E.; Weinhold, F. *The NBO 3.0 program manual*. Link to Gaussian programs, see ref 44.

(57) Compounds that were difficult to classify, COGTOH and COPFMP, are both Pb(IV) structures with coordination number 4. These were classified as holodirected.

(58) CSD code SOMMEM: Schneider, C.; Drager, M. *Organomet. Chem.* **1991**, *415*, 349−362.

(59) CSD code SARMUT: Hummel, H.-U.; Meske, H. *Z. Naturforsch. B* **1989**, *44*, 293−295.

(60) CSD code DOWYET: Preut, H.; Rohm, P.; Huber, F. *Acta Crystallogr.* **1986**, *C42*, 657−658.

(61) CSD code SANKUN: Engelhardt, L. M.; Furphy, B. M.; Harrowfeld, J. McB.; Patrick, J. M.; Skelton, B. W.; White, A. H. *J. Chem. Soc., Dalton Trans.* **1989**, 595−599.

(62) CSD code VIMMEJ: Veith, M.; Hans, J.; Stahl, L.; May, P.; Huch, V.; Sebald, Z. *Z. Naturforsch. B* **1991**, *46*, 403−424.

(63) CSD code DUPKAA: Clegg, W.; Little, I. R.; Straughan, B. P. *Acta Crystallogr.* **1986**, *C42*, 1319−1322.

(64) CSD code BIHWOE: Gaffney, C.; Harrison, P. G.; King, T. J. *J. Chem. Soc., Dalton Trans.* **1982**, 1061−1063.

(65) CSD code DEBGEW: Mak, T. C. W.; Yip, W.-H.; O'Reilly, E. J.; Smith, G.; Kennard, C. H. L. *Inorg. Chim. Acta* **1985**, *100*, 267−273.

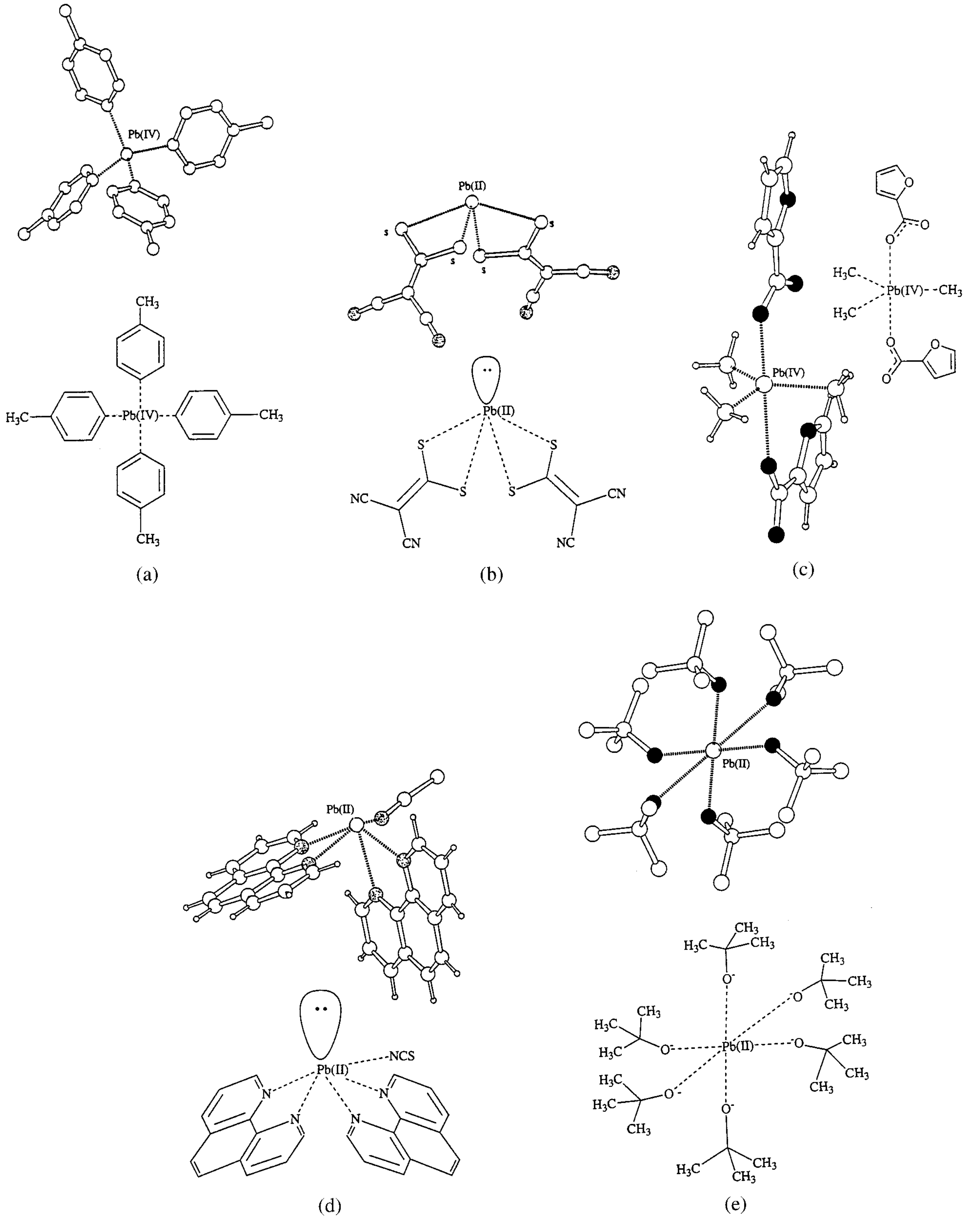

Figure 1. Examples for each type of geometry, holodirected and hemidirected, around the lead ion for coordination numbers (CN) 4 through 7. Unless marked differently, open circles represent carbon atoms, filled circles represent oxygen atom, and stippled circles represent nitrogen atoms. Hydrogen atoms are not included, for clarity, in a, e, g, or h. (a) Pb(IV), CN 4, SOMMEM[58]-tetra-*p*-tolyl-lead, holodirected tetrahedral geometry. (b) Pb(II), CN 4, SARMUT[59]-bis(tetraphenylarsonium) bis(1,1-dicyanoethylene-2,2-dithiolato-*S,S′*)lead(II), hemidirected tetrahedral geometry. (c) Pb(IV), CN 5, DOWYET[60]-(2-furoato)trimethyllead, holodirected trigonal bipyramidal geometry. (d) Pb(II), CN 5, SANKUN[61]-isothiocyanatobis-(1,10-phenanthroline-*N,N′*)lead(II) thiocyanate, hemidirected trigonal bipyramidal geometry. (e) Pb(II), CN 6, VIMMEJ[62]-hexakis(μ_2-*tert*-butyloxo-*O,O′*)digermanium lead(II), holodirected octahedral geometry. (f) Pb(II), CN 6, DUPKAA[63]-*catena*-((μ_3-crotonato-μ-*O*,μ-*O′*)(crotonato-μ-*O*,μ-*O′*)lead(II)), hemidirected octahedral geometry. (g) Pb(IV), CN 7, BIHWOE[64]-aquabis(diacetatodiphenyllead(IV)) benzene solvate, holodirected pentagonal bipyramidal geometry. (h) Pb(II), CN 7, DEBGEW[65]-*catena*-(μ_2-aquabis(phenoxyacetato-*O*)lead(II) bis(phenoxyacetato)lead(II), hemidirected pentagonal bipyramidal geometry.

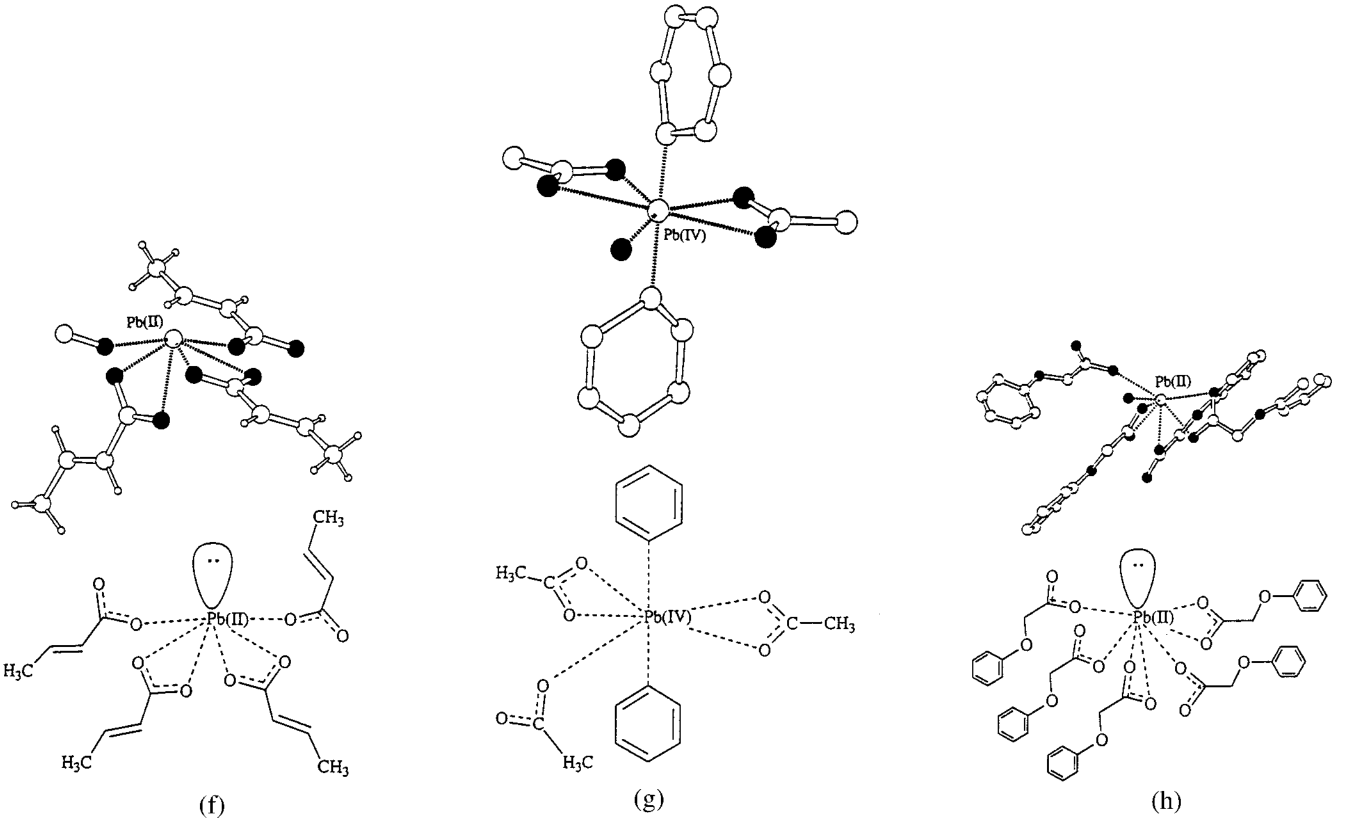

(f) (g) (h)

Figure 1. (continued)

Table 1. Percentage of Pb−Ligands in Each of the Two Main Geometries around the Metal Ion and the Percentage of Lead Complexes in Each Geometry in the Different Valence States

			% of Pb−X bonds with the given geometry							
coordination number	oxidation state	number and (%) of complexes[a]	C	N	O	S	Cl	Br	I	other
			(a) Pb(IV)							
holodirected ligands[b]										
4	IV	39 (39)	72		2	15		1		10
5	IV	19 (45)	62	10	16		5	6	1	
6	IV	10 (13)	26	17	17	7	33			
7	IV	3 (9)	25		75					
8	IV	3 (10)	8		92					
			(b)[c] Pb(II)							
holodirected ligands										
6[d]	II	47 (60)	1	8	14	10	10	7	20	
7	II	10 (29)	1	6	11	12		3		
8[e]	II	23 (80)		21	57	5	6			1
9	II	6 (100)		44	56					
10	II	12 (100)		13	85	4				
hemidirected ligands										
2	II	4 (100)	25	50	25					
3	II	24 (100)	1	30	28	26				15
4	II	61 (61)		26	30	38		0.5	0.5	5
5[f]	II	23 (55)		23	37	23	8	6	3	
6	II	21 (27)	1	8	15	4	2			
7	II	21 (62)		17	46	3			1	
8	II	3 (10)		2	6	3				

[a] Percentage of compounds with that coordination number. [b] No CSD entries for Pb(IV) for coordination numbers 2, 3, 9, or 10. [c] No entries found in the CSD for Pb(II) holodirected in coordination numbers 4 and 5. [d] JAWWIN has two lead ions each with different ligand atoms composition [e] One structure, PBACTH02, has an additional long (3.11 Å) Pb−O distance and therefore might be considered to have a coordination number of 9. [f] GEVWUZ has two lead ions, each with different ligand atom composition.

For divalent lead the situation is different. Despite the presence of a lone pair of electrons (which might be expected to favor a hemidirected geometry), *both* holodirected and hemidirected coordination geometries are found in the CSD, see Table 1. For coordination numbers from 2 to 5, *all* the Pb(II) compounds in the CSD show hemidirected geometries. On the other hand, for coordination numbers 9 and 10, *all* Pb(II) compounds in the CSD have holodirected geometries, although relatively few structures with these high coordination numbers were identified. For the intermediate coordination numbers (6, 7, and 8), *both* holodirected and hemidirected coordination geometries are reported for Pb(II) compounds in

Chart 1. Number of Structures Found in the CSD for Each Coordination Number for Pb(II) and Pb(IV)

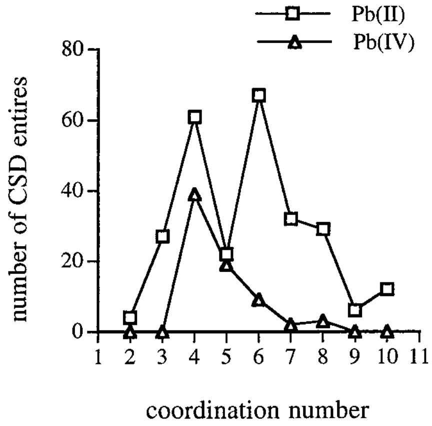

the CSD; the combined number of Pb(II) compounds with holodirected geometry at these three coordination numbers *exceeds* the number of compounds with hemidirected geometry, see Table 1b. These results imply that, when the number of coordinating ligands around Pb(II) is high, directional effects of the lone pair of electrons become less evident. This trend is probably to be expected on the basis of the "crowding" of the ligands as the coordination number increases.

(b) Identities of the Ligands. The relative percentage of structures found for each coordination number for Pb(II) and Pb(IV) is shown in Chart 1. There were 74 Pb(IV) compounds with coordination numbers from 4 to 8, but the majority have a coordination number of 4, with carbon or sulfur as covalently bound ligand, see Table 1a. As the coordination number of Pb(IV) increases, oxygen liganding is more favorable than that of carbon, although very few CSD entries were found at coordination numbers 7 and 8. Only one Pb(IV) compound in the CSD with coordination number 4 has a halogen ligand; this is in line with the ab initio pseudopotential findings of Kaupp and von Schleyer that there is a remarkable thermodynamic destabilization of four-coordinate Pb(IV) compounds with electronegative ligands.[50]

Pb(II) compounds were found in the CSD with coordination numbers from 2 to 10, but approximately 50% of these 255 structures have coordination numbers of 4 or 6. At all coordination numbers, $Pb^{II}-C$ bonds are rare. For the lower and higher coordination numbers of Pb(II) (2−4 and 9 and 10, respectively) there is a noticeable lack of halogen ligands in the reported crystal structure determinations (only 2 out of 107 entries contain at least one halogen ligand for these coordination numbers). Structures with coordination numbers 6−8, where both stereochemistries have been found, rarely occur with a hemidirected arrangement when the ligands are relatively soft halogens (Cl, Br, I), and when they do occur they are interspersed with hard oxygen and nitrogen ligands, see Table 1c. By contrast, hemidirected geometries can be found with sulfur ligands, even though sulfur is also considered to be soft. The relatively large number (21 out of 31) of hemidirected structures at coordination number 7 is somewhat surprising in view of possible ligand crowding. These structures generally contain a significant number of Pb−O bonds. For coordination number 8 only three hemidirected crystal structures were found (out of a total of 26), and all of these involved several Pb−O bonds.

There is a noticeable lack of water bound to either Pb(II) or Pb(IV). Only 23 structures were found in the CSD with lead-bound water molecules: *all* 23 were Pb(II) compounds, and most (14 in all) contained only a single lead-bound water molecule; none of these structures contained more than two water molecules bound to Pb(II).[66] This is in line with the low solubility of lead compounds in general.[67]

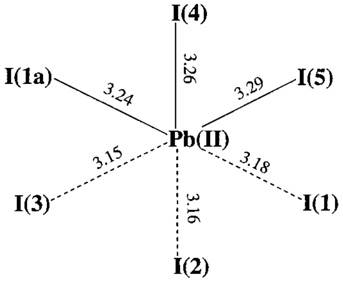

Figure 2. Pb- - -O distances in a holodirected hexacoordinated Pb(II) complex,[28] $[H_2N-C(I)=NH_2]_3PbI_5$. ESD values are 0.001−0.002 Å. Note that there are three shorter and three longer Pb- - -O distances.

Table 2. Comparison of the Mean (with ESD Values in Parentheses) Values for the Pb−Ligand Distances (in Å) for Complexes with a Holodirected Stereochemistry

	mean distance in Pb(II) complexes	mean distance in Pb(IV) complexes
N−Pb	2.62(11)	2.42(9)
O−Pb	2.53(15)	2.33(18)
S−Pb	3.02(18)	2.63(9)
Cl−Pb	2.88(8)	2.67(6)
Br−Pb	3.07(15)	2.81(13)
I−Pb	3.22(16)	

(c) $Pb^{II}-X$ Bond Lengths. The presence of a void in the angular distribution of ligands is usually taken as evidence for a stereochemically active lone pair of electrons, although some authors also require short $Pb^{II}-X$ distances to ligands opposite the void.[68] $Pb^{II}-X$ distances, however, can be significantly altered by the detailed structure of the liganding groups containing X and are also sensitive to the coordination number of the lead. Mean $Pb^{II}-X$ and $Pb^{IV}-X$ distances for compounds in the CSD that have a holodirected stereochemistry are listed in Table 2 as a function of coordination number. Distances from liganding atoms to lead are, on the average, 0.2 Å longer for Pb(II) than Pb(IV) compounds.

In holodirected Pb(II) complexes where all the ligands are identical (i.e., in homoleptic complexes)[40] and where the lead is located at the center of a symmetrical arrangement of liganding atoms, it seems justifiable to classify the lone pair of electrons as stereochemically inactive.[40] For example, in the main-group six-coordinate complex bis[hydrotris(3,5-dimethylpyrazolyl)borato]lead(II) the coordination geometry about the lead is a trigonally distorted octahedron with the lead ion at a center of inversion.[27] In this structure, all six $Pb^{II}-N$ distances are equal and the lone pair of electrons has no apparent directional effects on the angular distribution of the ligands or

---

(66) AQOHPB [CN5, hemidirected], CEJMIN [CN7, hemidirected], DEBGEW [CN7, hemidirected], FITMAW [CN7, hemidirected], FUFWEI [CN3, hemidirected], FUYDOS [CN8, holodirected], GEKTEV [CN7, holodirected], GEMJAJ [CN7, hemidirected], HABCES [CN7, hemidirected], HAKYOH [CN7, hemidirected], HEBDOX [CN8, holodirected], LAJDOP [CN 8, holodirected], PBACTH02 [CN8, holodirected] PBACTH10 [CN8, holodirected], PEFDAT [CN9, holodirected], PYCXPB [CN6, hemidirected], SEYFEH [CN 7, holodirected], VEYCUX [CN6, holodirected], WENVAM [CN8 hemidirected], WEWZON [CN7, holodirected], WIJYOD [CN7, holodirected], ZIKGAB [CN8, holodirected], ZUZSES [CN8, holodirected].

(67) Cotton, F. A.; Wilkinson, G. *Advanced Inorganic Chemistry,* 5th ed.; Wiley: New York, 1988.

(68) Hancock, R. D.; Shaikjee, M. S.; Dobson, S. M.; Boeyens, J. C. A. *Inorg. Chim. Acta* **1988**, *154*, 229−238.

Scheme 2. Interactions in Hemi- and Holodirected Geometries

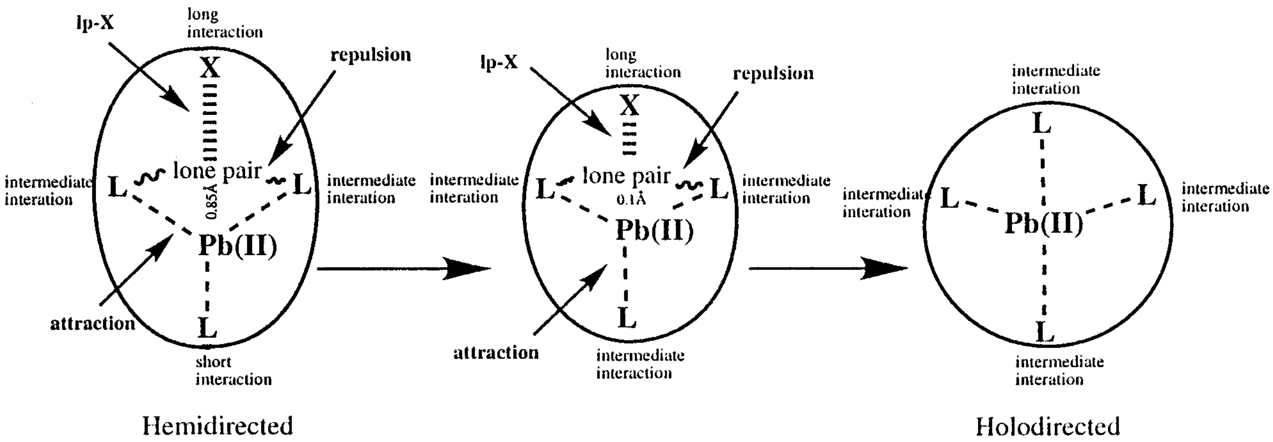

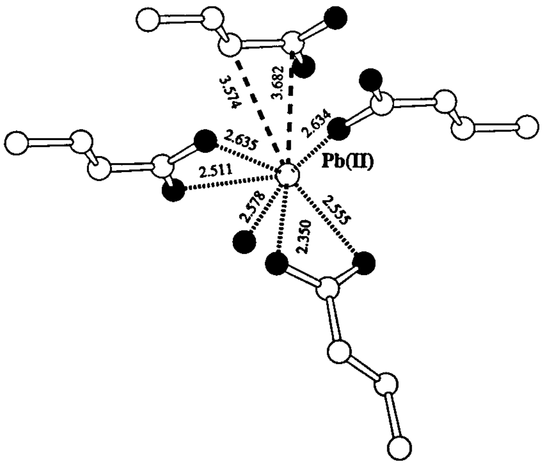

Figure 3. Lone pair interactions Pb−lp−C (dashed line) in DUPKAA-*catena*-[(μ-crotonato-*O*,*O*′)(crotonato-*O*,*O*′)lead(II)].[63] Pb−O indicated by dotted lines. Note the asymmetry in distances.

on the lead−ligand distances. In other homoleptic six-coordinate holodirected Pb(II) complexes, however, as noted by Brown,[69] there may be three adjacent short $\mathrm{Pb^{II}}$−X bonds and three adjacent long $\mathrm{Pb^{II}}$−X bonds (see Figure 2).[28] Such a specific pattern of differences in the bond lengths of holodirected homoleptic complexes has been attributed by various authors to repulsion involving a stereochemically active lone pair.[28,69] In holodirected heteroleptic complexes it may be difficult or even impossible to make an unambiguous designation of the specific consequences of the presence of a lone pair of electrons.[40]

For the hemidirected Pb(II) compounds in which the lone pair of electrons is presumed to be stereochemically active, the three-dimensional environment of the lone pair of electrons (lp) in the crystal structure is of significant interest. The differences between distances $\mathrm{Pb^{II}}$−X and $\mathrm{Pb^{II}}$−lp−X (the latter between Pb(II) and a ligand in the direction of the lone pair, opposite the $\mathrm{Pb^{II}}$−X direction) for structures in the CSD range from 0.3 to 1.2 Å, with no obvious effect of the identity of X; an example of this stereochemistry is shown in Figure 3. In this crystal structure the shortest $\mathrm{Pb^{II}}$−O distance is 2.35 Å [trans to the lone pair (axial)], while $\mathrm{Pb^{II}}$−O distances are longer, 2.63 Å, in the equatorial directions. In the direction of the lone pair of electrons, the $\mathrm{Pb^{II}}$−C distances are about 3.6 Å. This suggests that an ellipsoid of revolution, with the Pb(II) ion at one focus and the center of charge of the lone pair of electrons (lp) in the direction of the other focus, can be used as a model of the liganding, as diagrammed in Scheme 2. When this $\mathrm{Pb^{II}}$−lp distance is large, the coordination is viewed as hemidirected because $\mathrm{Pb^{II}}$−X bonds in one direction are very much shorter than those in the opposite direction. When the distance between foci is negligible, the coordination is holodirected, although the lone pair of electrons may or may not have stereochemical consequences. Thus in crystal structures there are two distinct observable effects of the presence of an active lone pair. In one, the ligands are hemidirected and there is a relatively large difference between the $\mathrm{Pb^{II}}$−X and $\mathrm{Pb^{II}}$−lp−X distances in the two axial directions. In the other, the ligands are holodirected and the difference is relatively small.

(d) Calculated Geometrical and Electronic Properties of Four-Coordinate Gas-Phase Lead Complexes. Since, when the coordination number is 4, only hemidirected Pb(II) compounds were found in the CSD, we decided to see if ab initio molecular orbital calculations could find any gas-phase holodirected complexes at this coordination number. To this end a variety of Pb(II) complexes were optimized using the MP2/LANL2DZ computational level; the LANL2DZ basis set was augmented with additional *d* functions on the heavy atoms.[45] The *x*,*y*, and *z* coordinates of all the optimized lead complexes are given in Table 4S of the Supporting Information. Coordination number 4 was chosen for these calculations because the resulting complexes were sufficiently small to allow higher level explorations of the potential energy surfaces for a greater number of Pb(II) complexes. All the natural polulation analysis (NPA) charges and orbital populations mentioned in this section are from the MP2 density. An NBO analysis was carried out in order to gain greater insight into the disposition of electrons in the various Pb(II) complexes.

We initially considered a variety of compounds containing formally neutral ligands around the divalent lead ion. Optimized structures of the $\mathrm{Pb^{II}}$−group 5A complexes $\mathrm{Pb^{II}{\cdot}4NH_3}$, $\mathrm{Pb^{II}{\cdot}4PH_3}$, $\mathrm{Pb^{II}{\cdot}4AsH_3}$, $\mathrm{Pb^{II}{\cdot}4SbH_3}$, and $\mathrm{Pb^{II}{\cdot}4BiH_3}$ are shown in Figure 4a, and the $\mathrm{Pb^{II}}$−group 6A complexes $\mathrm{Pb^{II}{\cdot}4OH_2}$, $\mathrm{Pb^{II}{\cdot}4SH_2}$, $\mathrm{Pb^{II}{\cdot}4SeH_2}$, and $\mathrm{Pb^{II}{\cdot}4TeH_2}$ are shown in Figure 4b. For a few of these compounds we searched for alternative local minima on the potential energy surfaces by altering the starting geometry, but the optimizations eventually returned to the structures in Figure 4. All nine of these complexes are hemidirected, although the exterior X−$\mathrm{Pb^{II}}$−X angles shown

---

(69) Brown, I. D. *J. Solid State Chem.* **1974**, *11*, 214−233.

(a)

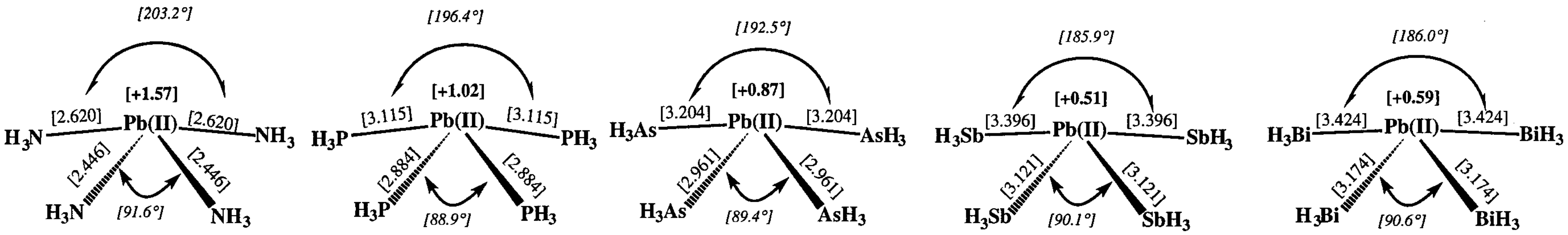

natural electron configuration	Pb:6s[1.89]6p[0.53]6d[0.01];$sp^{0.28}$	Pb:6s[1.91]6p[1.03]6d[0.02];$sp^{0.54}$	Pb:6s[1.89]6p[0.53]6d[0.01];$sp^{0.62}$	Pb:6s[1.91]6p[1.53]6d[0.03];$sp^{0.80}$	Pb:6s[1.91]6p[1.45]6d[0.03];$sp^{0.76}$
lone pair NBO	Pb:s [95.61%] p 0.05 [4.39%]	Pb:s [96.89%] p 0.03 [3.10%]	Pb:s [97.03%] p 0.03 [2.97%]	Pb:s [97.04%] p 0.03 [2.96%]	Pb:s [97.70%] p 0.02 [2.30%]
lone pair occupancy	[1.959]	[1.954]	[1.950]	[1.947]	[1.940]
% NBO on Pb(II) (short bonds)	5.3%	14.3%	16.8%	22.5%	21.3%

(b)

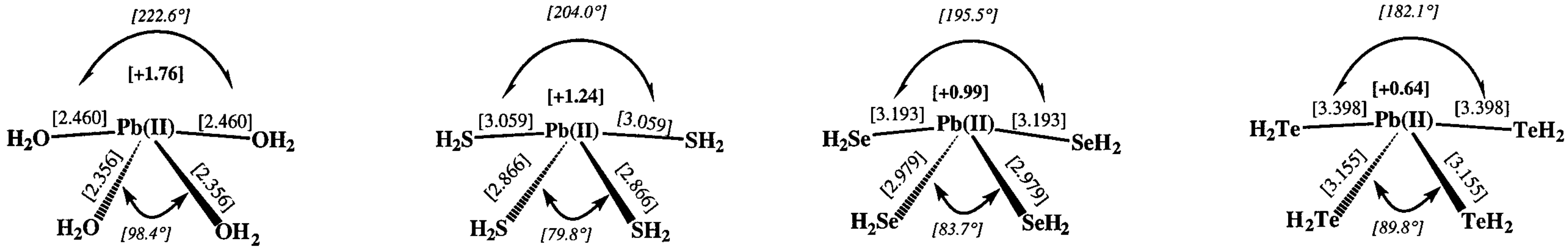

natural electron configuration	Pb:6s[1.91]6p[0.31]6d[0.01];$sp^{0.16}$	Pb:6s[1.94]6p[0.79]6d[0.02];$sp^{0.41}$	Pb:6s[1.94]6p[1.03]6d[0.03];$sp^{0.53}$	Pb:6s[1.93]6p[1.37]6d [0.03];$sp^{0.71}$
lone pair NBO	Pb: s [97.35%] p 0.03 [2.65%]	Pb: s [98.16%] p 0.02 [1.84%]	Pb: s [98.09%] p 0.02 [1.91%]	Pb: s [97.99%] p 0.02 [2.00%]
lone pair occupancy	[1.960]	[1.965]	[1.965]	[1.961]
% NBO on Pb(II) (short bonds)		10.4%	13.8%	19.0%

Figure 4. Geometries from ab initio molecular orbital calculations for (a) complexes $Pb^{II}\cdot4NH_3$, $Pb^{II}\cdot4PH_3$, $Pb^{II}\cdot4AsH_3$, $Pb^{II}\cdot4SbH_3$, and $Pb^{II}\cdot4BiH_3$ and (b) $Pb^{II}\cdot4H_2O$, $Pb^{II}\cdot4H_2S$, $Pb^{II}\cdot4H_2Se$, and $Pb^{II}\cdot4H_2Te$. [ ] = MP2/LANL2DZ+*d* optimization, MP2 charges. The electron distribution is indicated for each structure.

Table 3. Energy Difference, ΔE, between Hemidirected (Local Minima) and Holodirected (Constrained) Forms of Some Four-Coordinate Gas-Phase Complexes

complex	ΔE_a (kcal/mol) from hemidirected to holodirected geometry
$Pb^{II}\cdot 4NH_3$	+12.1
$Pb^{II}\cdot 4PH_3$	+9.8
$Pb^{II}\cdot 4OH_2$	+7.7
$Pb^{II}\cdot 4SH_2$	+9.5
$Pb^{II}\cdot 4TeH_2$	+5.5
$Pb^{II}\cdot 4OH^-$	+28.6
$Pb^{II}\cdot 4SH^-$	+4.9
$Pb^{II}\cdot 4TeH^-$	+1.6
$Pb^{II}\cdot 4F^-$	+6.2

[a] $\Delta E = E$(constrained and holodirected) − E(fully optimized and hemidirected) with energies from the MP2/LANL2DZ+*d* computational level.

in Figure 4 vary from about 182 to 223°. In all cases NPA charges show a transfer of electrons to the lead from the ligands. The least amount of charge is transferred to the Pb(II) when the ligands are OH_2, NH_3, and SH_2, and all three of these complexes have exterior X−Pb^{II}−X angles in excess of 200°. An analysis of the natural bond orbitals (NBOs) shows that the Pb(II) lone pair orbital is predominantly 6s but is slightly polarized by a small 6p contribution, e.g. 4.4% and 2.6% for $Pb^{II}\cdot 4NH_3$ and $Pb^{II}\cdot 4OH_2$, respectively. The lowering in energy, ΔE, that these complexes experience by adopting a hemidirected arrangement of ligands rather than a holodirected arrangement, where the ligands are as far apart as possible, was estimated by reoptimizing their geometry with the liganding atoms secured in a tetrahedral arrangement around the Pb(II) and equidistant from it. The results are shown in Table 3. The values of ΔE for the complexes with the ligands NH_3, PH_3, OH_2, and SH_2, which include the most common liganding atoms from the CSD, vary over a relatively narrow range, 7.7−12.1 kcal/mol.

As can be seen from Chart 2a, the net (NPA) positive charge on the divalent lead ion generally decreases in going down the Pb^{II}−group 5A and Pb^{II}−group 6A complexes, showing a greater transfer of electron density from the ligands to the lead as the electronegativity of the ligand decreases. The transfer of electrons is primarily into the 6p orbitals on the lead as shown by the increasing the 6p/6s population ratio, see Chart 2b, although the p composition of the NBO lone pair orbital actually decreases slightly (see Figure 4). The primary structural consequence of the greater lead p population is a decrease in the exterior X−Pb^{II}−X angle, see Chart 2c and Figure 4, suggesting some tendency toward a more tetrahedral (holodirected) arrangement of the ligands around the lead. Kaupp and von Schleyer[50] noted a similar effect in their study of covalent bonding in the holodirected four-coordinate Pb(IV) compounds $R_nPb^{IV}X_{4-n}$ (R = H, CH_3; X = F, Cl; n = 0−4).

In the Pb(II) complexes in Figure 4, the calculated lead−ligand distances opposite the lone pair are consistently found to be shorter than others, and the difference in the distance between the two long and two short Pb^{II}−X bonds increases going down either group, as also found in the CSD. For all the calculated structures in Figure 4 the X−Pb^{II}−X angles involving the two short Pb^{II}−X bonds are less than 100° and often less than 90°, suggesting significant p character in these bonds; the larger angles involving the longer bonds imply more s character in the bonding. An analysis of the NBOs of $Pb^{II}\cdot 4NH_3$ finds the p/s ratio of the lead contribution to the shorter bonds to be approximately 4.5 times larger than that to the longer bonds.

We also investigated Pb(II) complexes with charged ligands (where ligand−ligand repulsion is more significant). The optimized Pb^{II}−group 6A complexes $Pb^{II}\cdot 4OH^-$, $Pb^{II}\cdot 4SH^-$, $Pb^{II}\cdot 4SeH^-$, and $Pb^{II}\cdot 4TeH^-$ shown in Figure 5a are each hemidirected, although the exterior X−Pb^{II}−X angles vary from 215° for $Pb^{II}\cdot 4OH^-$ to 161° for $Pb^{II}\cdot 4TeH^-$. The Pb^{II}−group 6A complexes with charged and uncharged ligands show that more electron density is transferred to the lead when the ligands carry a formal negative charge but that the population of the 6s orbital on the Pb(II) is lower, resulting in greater 6p/6s population ratios and significantly smaller exterior X−Pb^{II}−X angles. The lone pair Pb(II) orbital consistently has greater p character when the ligands are charged. A reoptimization of the $Pb^{II}\cdot 4OH^-$ complex with the oxygen atoms in a tetrahedral arrangement around the Pb(II) and all lead−oxygen distances constrained to be equal yielded a structure that is 28.6 kcal/mol higher in energy than the completely optimized structure, see Table 3. This energy difference is nearly 4 times larger than the result of applying the same distortions to the corresponding water complex. In the hemidirected form of $Pb^{II}\cdot 4OH^-$, however, O···H interactions between hydroxyl groups apparently stabilize this form of the complex, see Figure 5a in the Supporting Information. The tetrahedral forms of $Pb^{II}\cdot 4SH^-$ and $Pb^{II}\cdot 4TeH^-$ are only 4.9 and 1.6 kcal/mol higher in energy, respectively, than their fully optimized forms. These values are smaller than the corresponding values for the neutral species, which correlates with the smaller exterior X−Pb^{II}−X angles for the negatively charged ligands. In all of these complexes the two Pb^{II}−ligand distances opposite the lone pair of electrons are again found to be shorter (as in the CSD structures), but the X−Pb^{II}−X angles involving these ligands are somewhat larger than those found with the neutral ligands, ranging from 101.7 to 108.3°. The NBOs of $Pb^{II}\cdot 4OH^-$ are such that the p/s ratio of the lead contribution to the shorter bonds is about 4.0 times larger than the lead contribution to the longer bonds.

The Pb^{II}−group 7A complexes $Pb^{II}\cdot 4X^-$ were also optimized, see Figure 5b. The $Pb^{II}\cdot 4F^-$ complex, which involves small hard fluorine ion ligands, remains hemidirected, despite substantial electrostatic repulsion between the highly charged fluoride ions; NPA charges on the fluoride ions, associated with the Pb^{II}−F short and long bonds, are −0.83 and −0.88, respectively, indicating that relatively little charge is transferred to the lead. Although the NBO lone pair orbital on the lead remains predominantly s, it has 9.2% p character, and we found that $Pb^{II}\cdot 4F^-$ can be viewed as tending toward a complex between $Pb^{II}F_2$ and two separate fluoride ions. A reoptimization of $Pb^{II}\cdot 4F^-$ with the fluoride ions in a tetrahedral arrangement and with all lead−fluorine distances equal gives a structure which is only 6.2 kcal/mol higher in energy than the optimized form shown in Figure 5b. The remaining three Pb^{II}−halogen ion complexes involve much larger and softer ions (Cl^-, Br^-, and I^-) and are found to be holodirected with all four Pb^{II}−X bond lengths equal in each complex. The NBO lone pair orbital has no polarizing p component. All four Pb^{II}−X bonds in these complexes are clearly ionic, but the ionic character of the bonds decreases as the atomic number of the halogen ligand increases. The NPA charges on the halogens in these three complexes are less negative than that on the fluorine in $Pb^{II}\cdot 4F^-$, suggesting less ligand−ligand repulsion.

Insight into the changes that occur in going from a holodirected to a hemidirected arrangement of ligands was obtained by artificially fixing one of the Cl−Pb^{II}−Cl angles in $Pb^{II}\cdot 4Cl^-$ and allowing the remainder of the structure to optimize. This angle was then altered and the procedures repeated for various

Chart 2. Values for Different Rows in the Periodic Table of (a) the NPA Positive Charge on Pb(II), (b) n in sp^n-Hybridized Orbitals, and (c) the External X−Pb^{II}−X Angle

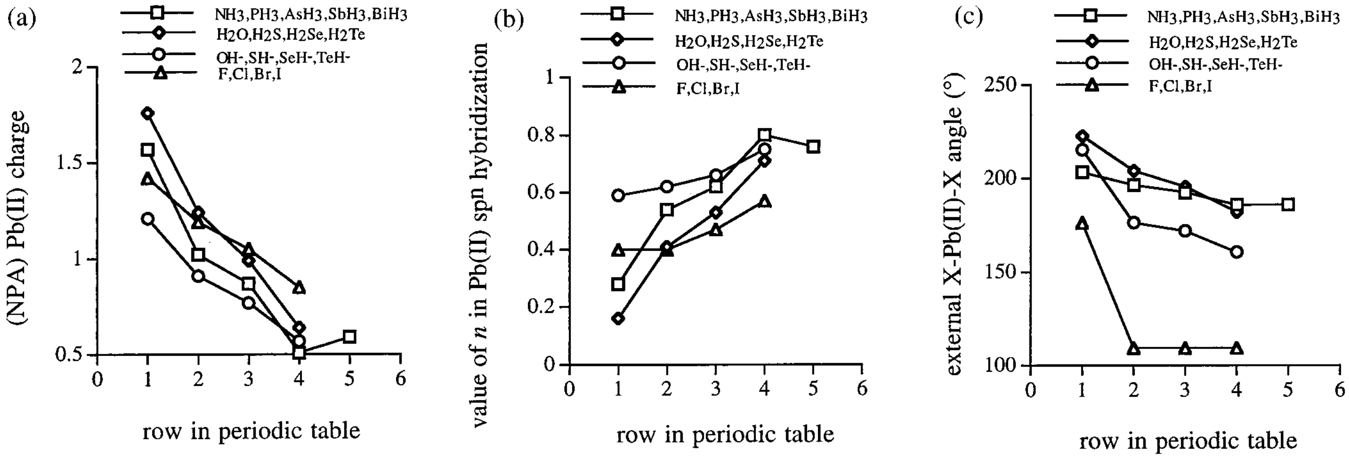

values near the ideal tetrahedral angle of 109.5°. In Table 4 we list several properties of Pb^{II}•4Cl$^-$ as a function of the Cl−Pb^{II}−Cl angle. As this angle is increased above 109.5°, the contribution of the lead orbital to the NBOs associated with the pair of shorter Pb^{II}−Cl bonds increases, indicating somewhat greater covalent character.[55,56] Furthermore, the p/s ratio of this lead (hybrid) orbital increases dramatically, resulting in a smaller angle between these two Pb^{II}−Cl bonds. On the other hand, the contribution of the lead to the NBO that is associated with the pair of longer Pb^{II}−Cl bonds decreases, and these bonds become even more ionic. For angles greater than about 135°, the orbitals associated with these longer bonds effectively appear as lone pair orbitals localized on the chlorines. The overall transfer of electrons to the lead p orbital increases as the Cl−Pb^{II}−Cl angle increases, and the NBO lone pair orbital gains a small amount of p character.

For comparison, we examined the transfer of charge in some tetravalent lead complexes. The structures of Pb^{IV}•4OH$_2$ and Pb^{IV}•4Cl$^-$ were optimized and are shown in Figure 6.[71] As expected, both structures are holodirected and the Pb−X bond lengths are shorter than in the corresponding Pb(II) complexes also found in the CSD search. Although the Pb^{IV}−X bonds in these complexes are essentially ionic, they have much greater covalent character than the Pb^{II}−X bonds in the corresponding Pb(II) complexes, see Figures 4−6. Significant charge is transferred to the lead, and the 6p/6s population ratios are higher in Pb^{IV}•4H$_2$O and Pb^{IV}•4Cl$^-$ than those found in the corresponding Pb(II) structures, due to the low 6s population in this form of lead that lacks a lone pair of electrons.

(e) Effects of the Identities of the Ligands on the Coordination Geometry. Since at coordination numbers 6 and 7 both hemidirected and holodirected geometry can be found in structures in the CSD, we investigated the types of ligands found for each (see Table 5). For coordination numbers 6 and 7 there is a definite tendency for oxygen and nitrogen to be involved in hemidirected geometry and for halogens (not including fluorine) to be involved in holodirected geometry. In addition there are more hemi- than holodirected structures in which the ligand atoms are connected to each other, for example, as part of a ring system, with two groups on the same molecule coordinated to the lead (chelated), or by a bidentate interaction with the lead (two atoms separated by one atom, as in carboxylates, bonded to the lead), see Table 5.

(f) Effects of Steric Overcrowding on the Coordination Geometry. The association of high coordination numbers with holodirected coordination geometry about Pb(II) suggests that steric overcrowding is an important contributing factor in determining the hemi- or holodirected nature of a Pb(II) compound. Reger and co-workers[27] in their study of the six-coordinate crystal structures of bis[hydrotris(pyrazolyl)borato]-lead(II) [HB(pz)$_3$]$_2$Pb^{II} and its 3,5-analogue [HB(3,5-Me$_2$pz)$_3$]$_2$Pb^{II} have provided convincing evidence that this is the case. For each of these compounds the lead is bound to two complexing molecules via a total of six pyrazole rings (three from each molecule). The former structure is hemidirected, while the latter is holodirected. An examination of these structures (shown in Figure 7) indicates that the ligands (apart from the additional methyl groups) have nearly the same conformations. The difference comes when the two molecules adjust themselves around the Pb(II) each with three points of contact (one of the nitrogen atoms in each of the three pyrazole rings) to the metal ion. In the dimethyl complex interligand interactions between methyl groups on different molecules do not allow the two ligands to approach each other as closely as when the methyl groups are missing, and therefore the ligands fill more space around the Pb(II) (becoming holodirected). As a result, a judicious selection of ligand geometry can be used to design complexing agents that allow the lone pair of electrons on Pb(II) to be stereochemically active or that effectively suppress this activity.[6]

(g) Effects of the Sizes and Charge Distribution of the Ligands on the Coordination Geometry. Since a number of divalent lead compounds in the CSD have carboxylate ligands, we also studied the structure of the Pb^{II}•4OCHO$^-$ complex,

---

(70) It should be pointed out that the calculated structures of the complexes Pb^{II}•2X$^-$ and Pb^{II}•3X$^-$ [X = Cl, Br, I] are, respectively, *not* linear or planar, indicating that the lone pair is stereochemically active in these two- and three-coordinate structures. Thus, there are currently no known experimental or calculated holodirected two- or three-coordinate Pb(II) complexes. The overall 6p/6s population ratios in the hemidirected complex Pb^{II}•4F$^-$ and the holodirected complex Pb^{II}•4Cl$^-$ are nearly the same, 0.40. However, more charge is transferred to the lead in Pb^{II}•4Cl$^-$ and both the 6s and 6p populations are greater in the holodirected complex. In the constrained tetrahedral form of Pb^{II}•4F$^-$, less charge is transferred to the lead and the 6p/6s population ratio is much smaller, 0.24.

(71) The complexes Pb^{IV}•2Cl$^-$ and Pb^{IV}•3Cl$^-$ are calculated to be linear and planar, respectively.

(72) Only one optimized structure of Pb^{II}•3OCHO$^-$ was located, and it has three monodentate Pb^{II}−carboxylate interactions; three local minima of Pb^{II}•2OCHO$^-$ were found (two monodentate, two bidentate, or one mono- and one bidentate interactions). Examples of both mono- and bidentate interactions are found in the CSD, although not at coordination number 4.

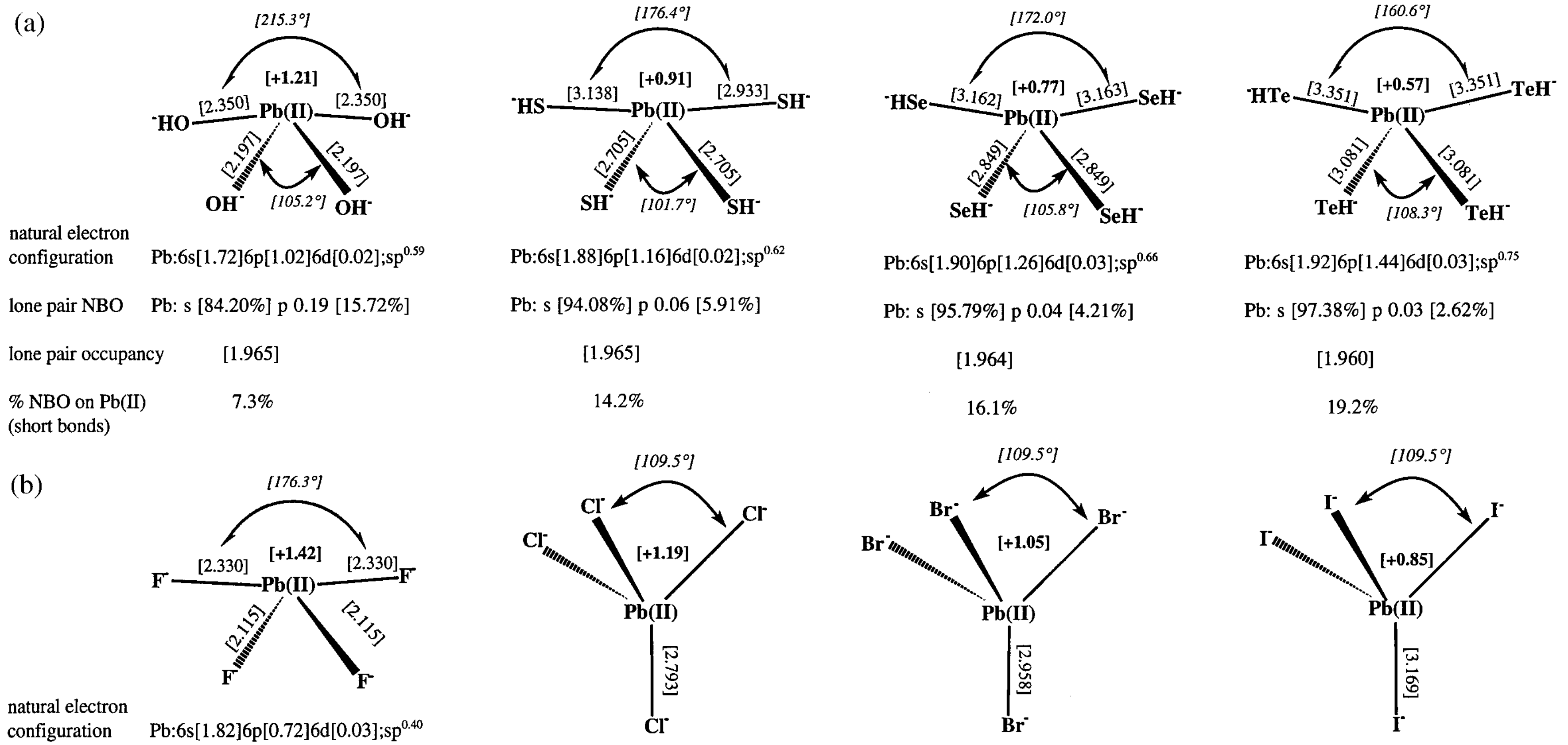

(a)

natural electron configuration	Pb:6s[1.72]6p[1.02]6d[0.02];sp$^{0.59}$	Pb:6s[1.88]6p[1.16]6d[0.02];sp$^{0.62}$	Pb:6s[1.90]6p[1.26]6d[0.03];sp$^{0.66}$	Pb:6s[1.92]6p[1.44]6d[0.03];sp$^{0.75}$
lone pair NBO	Pb: s [84.20%] p 0.19 [15.72%]	Pb: s [94.08%] p 0.06 [5.91%]	Pb: s [95.79%] p 0.04 [4.21%]	Pb: s [97.38%] p 0.03 [2.62%]
lone pair occupancy	[1.965]	[1.965]	[1.964]	[1.960]
% NBO on Pb(II) (short bonds)	7.3%	14.2%	16.1%	19.2%

(b)

natural electron configuration	Pb:6s[1.82]6p[0.72]6d[0.03];sp$^{0.40}$	Pb:6s[1.96]6p[0.78]6d[0.02];sp$^{0.40}$	Pb:6s[1.96]6p[0.92]6d[0.02];sp$^{0.47}$	Pb:6s[1.96]6p[1.12]6d [0.02];sp$^{0.57}$
lone pair NBO	Pb: s [90.62%] p 0.10 [9.24%]	Pb: s [100%] p 0.00 [0.00%]	Pb: s [100%] p 0.00 [0.00%]	Pb: s [100%] p 0.00 [0.00%]
lone pair occupancy	[1.971]	[1.964]	[1.963]	[1.961]
% NBO on Pb(II)	6.1%	5.2%	6.7%	8.8%

Figure 5. Geometries from ab initio molecular orbital calculations for (a) complexes $Pb^{II}\cdot 4OH^-$, $Pb^{II}\cdot 4SH^-$, $Pb^{II}\cdot 4SeH^-$, and $Pb^{II}\cdot 4TeH^-$ and (b) $Pb^{II}\cdot 4F^-$, $Pb^{II}\cdot 4Cl^-$, $Pb^{II}\cdot 4Br^-$, and $Pb^{II}\cdot 4I^-$. [ ] = MP2/LANL2DZ+*d* optimization, MP2 charges. The electron distribution is indicated for each structure.

Table 4. Properties of $\mathrm{Pb^{II}\cdot 4Cl^{-}}$ as a Function of the $\mathrm{Cl-Pb^{II}-Cl}$ Angle

	$\mathrm{Cl-Pb^{II}-Cl}$ angle[a]			
	110°	120°	130°	135°
E_{REL} (kcal/mol)[b,c,d]	0.00	+0.09	+0.28	+0.42
% Pb in NBO (long Pb−Cl bonds)[c]	5.16	4.29	3.72	3.52
% Pb in NBO (short Pb−Cl bonds)[c]	5.28	6.37	7.40	7.88
% p in lone pair NBO orbital[c]	0.00	0.27	0.83	1.18
long $\mathrm{Pb^{II}-Cl}$ bond distance (Å)[c]	2.795	2.842	2.871	2.880
short $\mathrm{Pb^{II}-Cl}$ bond distance (Å)[c]	2.790	2.740	2.704	2.689
$\mathrm{Cl-Pb^{II}-Cl}$ bond angle (deg)[c,e]	109.1	103.5	100.6	99.8
$\mathrm{Pb^{II}}$ positive charge[c,f]	+1.193	+1.190	+1.183	+1.178
sp^non $\mathrm{Pb^{II}}$[c](value of n)	0.398	0.403	0.410	0.415

[a] This angle is between the two long $\mathrm{Pb^{II}-Cl}$ bonds. [b] Energy relative to the value at 110°. [c] MP2/LANL2DZ+*d* energies, distances, and charges. [d] The nuclear repulsion energy increases dramatically as the angle increases. [e] This angle is between the two short $\mathrm{Pb^{II}-Cl}$ bonds. [f] NPA charges, MP2 density.

optimizing it by ab initio molecular orbital calculations. This provides an example of a complex with oxygen directly bound to the lead, but in which the ligands are bulky. Furthermore, these ligands contain additional oxygen atoms that carry substantial charge with the potential for increased ligand−ligand repulsion. The resulting structure is still hemidirected, see Figure 8, and all four $\mathrm{Pb^{II}}$−carboxylate interactions are monodentate; the shortest distance between Pb(II) and a nonbonded oxygen atom is nearly 3.5 Å.[72] There is a significant asymmetry in the two longer $\mathrm{Pb^{II}-O}$ distances in $\mathrm{Pb^{II}\cdot 4OCHO^{-}}$, a result of H···O interactions among the carboxylate groups, see Figure 5b in the Supporting Information. Although the series of complexes $\mathrm{Pb^{II}\cdot 4OH_2}$, $\mathrm{Pb^{II}\cdot 4OH^{-}}$, and $\mathrm{Pb^{II}\cdot 4OCHO^{-}}$ all are hemidirected, their exterior $\mathrm{O-Pb^{II}-O}$ angles, 223, 215, and 195°, respectively, vary over a range of nearly 30°; $\mathrm{Pb^{II}-O}$ distances vary from 2.20 to 2.48 Å. Thus, details of the geometry of the ligands, as well as their distribution of charges and any interactions in which they are involved, can have dramatic effects on the external angle, even if the ligand atom is the same.

(h) Effects of Interactions between the Ligands on the Coordination Geometry. To investigate interligand interactions by molecular orbital calculations, the complexes $\mathrm{Pb^{II}\cdot 4Br^{-}}$, $\mathrm{Pb^{II}\cdot 4BrH}$, and $\mathrm{Pb^{II}\cdot 4BrK}$ were optimized at the MP2/LANL2DZ level, where the LANL2DZ basis set was augmented by additional polarization functions (*d* on Pb(II), Br; *p* on K). The resulting structures are shown in Figure 9. Unlike $\mathrm{Pb^{II}\cdot 4Br^{-}}$, $\mathrm{Pb^{II}\cdot 4BrH}$ has a hemidirected coordination geometry. Thus, even if the directly liganded atoms are the same, it is possible to have significantly different stereochemistries. It may be noted that the net NPA charge on the bromines in $\mathrm{Pb^{II}\cdot 4BrH}$ is much less than that in $\mathrm{Pb^{II}\cdot 4Br^{-}}$, effectively reducing ligand−ligand repulsion. This difference in stereochemistry is not entirely a function of the charge on the ligand since, as noted previously, $\mathrm{Pb^{II}\cdot 4OH_2}$, $\mathrm{Pb^{II}\cdot 4OH^{-}}$, and $\mathrm{Pb^{II}\cdot 4OCHO^{-}}$ are all calculated to be hemidirected in the gas phase. Furthermore, the structure of $\mathrm{Pb^{II}\cdot 4BrK}$, in which the NPA charges on the bromines are comparable to those in $\mathrm{Pb^{II}\cdot 4Br^{-}}$, is similarly hemidirected, although the exterior $\mathrm{Br-Pb^{II}-Br}$ angle is approximately 10° smaller than that in $\mathrm{Pb^{II}\cdot 4BrH}$. It would appear that the structure of $\mathrm{Pb^{II}\cdot 4BrK}$ is such as to optimize the number of possible potassium−bromine interactions, see Figure 5c−e in the Supporting Information, thereby favoring a hemidirected stereochemistry. A similar situation was observed in the case of $\mathrm{Pb^{II}\cdot 4OH^{-}}$.

(i) Effects of Mixing Ligands on the Coordination Geometry about Pb(II). To assess the effects of mixing ligands that favor hemidirected with those that favor holodirected geometries, we inspected the stereochemistries of the chimeric complexes $\mathrm{[Pb^{II}Cl}_n\mathrm{(OCHO)}_{4-n}]^{2-}$, since the calculated structure of $\mathrm{Pb^{II}\cdot 4OCHO^{-}}$ is hemidirected while that of $\mathrm{Pb^{II}\cdot 4Cl^{-}}$ is holodirected. These calculations were performed without the additional *d*-functions on the heavy atoms to reduce the required computer time. The results are also shown in Figure 8. As the number of softer $\mathrm{Cl^{-}}$ ligands is increased in this series, the coordination geometry of the complex clearly becomes more holodirected. This is accompanied by an increase in the charge transferred to the lead. The populations of both the 6s and 6p orbitals increase as does the 6p/6s ratio.

Discussion and Conclusion

There are two general structural categories of Pb(II) compounds in the CSD: holodirected and hemidirected. These are distinguished by the disposition of ligands around the metal ion. In the hemidirected form there is a void in the liganding which is not found with holodirected geometry. Ab initio MP2/LANL2DZ molecular orbital calculations find the same two types of stereochemistry with four-coordinate gas-phase Pb(II) complexes, confirming this classification.

Lead shows a wide variety of coordination numbers. Our analyses of crystal structures in the CSD finds Pb(IV) compounds with coordination numbers from 4 to 8, but the majority have coordination number 4, and all are holodirected. On the other hand, Pb(II) can bind as few as two and as many as 10 ligands, with preferred coordination numbers of 4 and 6. Hemidirected complexes are found for the lower coordination numbers of Pb(II) (2−5), while holodirected stereochemistries are observed for its higher coordination numbers (9−10) where ligand overcrowding is apparently a significant issue. At intermediate Pb(II) coordination numbers (6−8) crystal structures with both holodirected and hemidirected stereochemistries are found. Although no examples of four-coordinate holodirected Pb(II) compounds were found in the CSD, MP2/LANL2DZ optimizations predict that Pb(II) complexes with large soft ions ($\mathrm{Cl^{-}}$, $\mathrm{Br^{-}}$, and $\mathrm{I^{-}}$) as ligands should be holodirected. In line with this prediction, at coordination numbers 6 through 8 compounds in the CSD with significant numbers of (soft) Cl, Br, or I ligands are found to be holodirected. Optimizations of other four-coordinate Pb(II) complexes with a wide variety of ligands, charged and uncharged, resulted only in hemidirected geometries, in general agreement with the results of the CSD search.

One might expect that specific atoms bound to Pb(II) would have a major influence on the stereochemistry (hemi- or holodirected) of the compound. To some extent this is observed. As noted above, hemidirected Pb(II) arrangements are rarely found in the presence of a significant number of Cl, Br, or I ligands, while there is a tendency for oxygen and nitrogen to be involved in hemidirected geometries at intermediate coordination numbers. However, at coordination number 6 there are examples of both holo- and hemidirected compounds in which the liganding atoms are six oxygen or six nitrogen atoms. An inspection of these structures from the CSD suggests that interligand repulsion is responsible for the geometry of at least some of the holodirected compounds.[27] On the other hand, ab initio calculations find that $\mathrm{Pb^{II}\cdot 4Br^{-}}$, which has four negatively charged bromide ions presumably repelling each other, is holodirected, while $\mathrm{Pb^{II}\cdot 4BrH}$ and $\mathrm{Pb^{II}\cdot 4BrK}$, in which the effect of the bromide ion has been counteracted to some extent by covalent bond formation or by the presence of cations, are both hemidirected. These observations imply that altering the

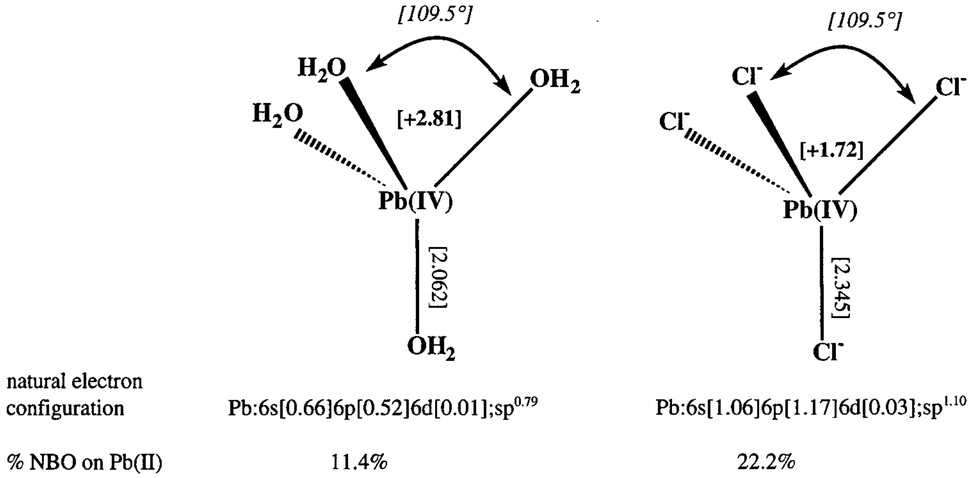

Figure 6. Geometries from ab initio molecular orbital calculations for the complexes $Pb^{IV}\cdot 4H_2O$ (**10**) and $Pb^{IV}\cdot 4Cl^-$ (**11**). [ ] = MP2/LANL2DZ+*d* optimization, MP2 charges.

Table 5. Percentages of Various Types of Ligands at Coordination Numbers 6 and 7 for Pb(II)

	coordination number 6		coordination number 7	
	hemidirected	holodirected	hemidirected	holodirected
no. of entries	21	47	21	10
ligand type				
O, N	82	33	92	53
S	12	14	7	38
Cl, Br, I	6	53	1	9
ring, chelate bidentate	47	9	69	45

effective charge on the liganding atoms or having attractive interactions among the ligands can disrupt the stereochemistry. Thus, interactions (repulsive or attractive) among the ligands play an essential role in determining the stereochemistry of Pb(II) complexes.

Our molecular orbital calculations provide some valuable insight into (four-coordinate) Pb(II) complexes.

(1) Converting a fully optimized hemidirected complex into a constrained holodirected complex, i.e., making the lone pair stereochemically inactive, requires approximately 8–12 kcal/mol for the simple formally uncharged ligands NH_3, PH_3, OH_2, and SH_2. Interactions between ligands can increase or decrease this energy cost significantly. For example, for $Pb^{II}\cdot 4OH^-$ where there are interligand H···O attractive interactions, the required energy is nearly 29 kcal/mol.

(2) The NBO associated with the lone pair of electrons on the Pb(II) in the hemidirected complexes in Figures 4 and 5 is primarily 6s, polarized by a surprisingly small p contribution that is responsible for the void in the distribution of ligands; the lone pair orbitals in the holodirected complexes $Pb^{II}\cdot 4X^-$ (X = Cl, Br, I) are entirely s in character. We find, in preliminary studies, that $Sn^{II}\cdot 4Cl^-$ is hemidirected, as expected, since the stereochemical activity of the lone pair is known to be enhanced for smaller cations.[28]

(3) For all the hemidirected Pb(II) complexes we studied, NPA charge is transferred from the ligands to the lead. As the electronegativity of the liganding group decreases, more charge is transferred to the 6p orbitals on the lead. This added charge does *not* increase the p character of the lone pair orbitals, but increases the p character of the $Pb^{II}-X$ bonding orbitals, resulting in a decrease in the exterior $X-Pb^{II}-X$ angles.

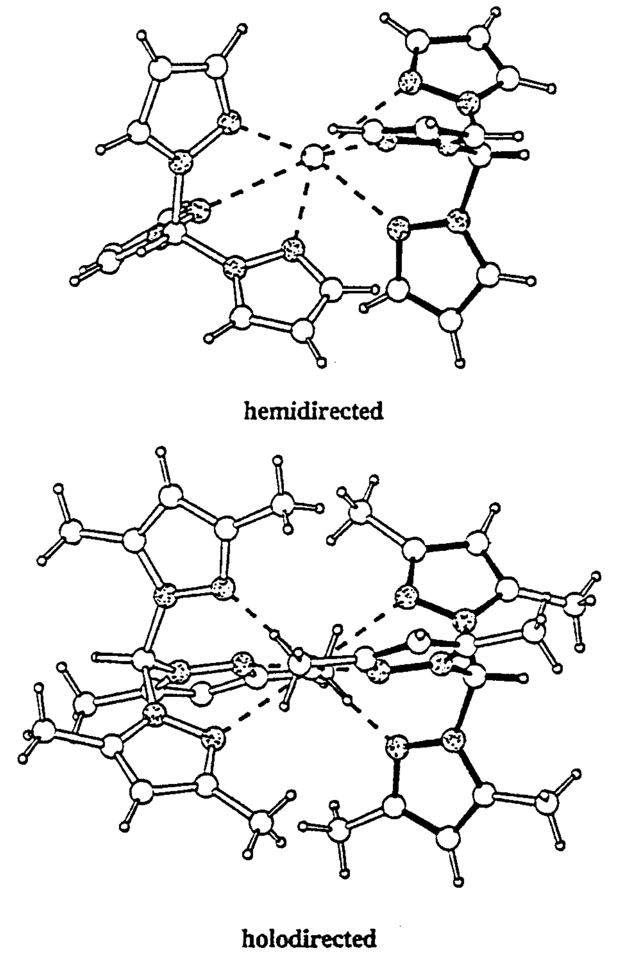

Figure 7. Comparison of the structures of the $[HB(pz)_3]_2Pb^{II}$ (hemidirected) and $[HB(3,5\text{-}Me_2pz)_3]_2Pb^{II}$ (holodirected).[41] One molecule of complexing agent is denoted by filled bonds. Note that the complexing agent has the same configuration in both cases. Methyl groups in the latter prevent hemidirected geometry for steric reasons.

(4) The two shorter $Pb^{II}-X$ bonds in the hemidirected four-coordinate complexes have greater covalent character than do the two longer $Pb^{II}-X$ bonds. In fact, the NBOs suggest that $Pb^{II}\cdot 4F^-$ can be considered as a complex between $Pb^{II}F_2$ and two separate fluoride ions.

Our analysis suggests that the "normal" arrangement of ligands around Pb(II) is hemidirected, although the "size" of the void (e.g. the exterior $X-Pb^{II}-X$ angle for four-coordinate complexes) in the distribution of ligands is very sensitive to

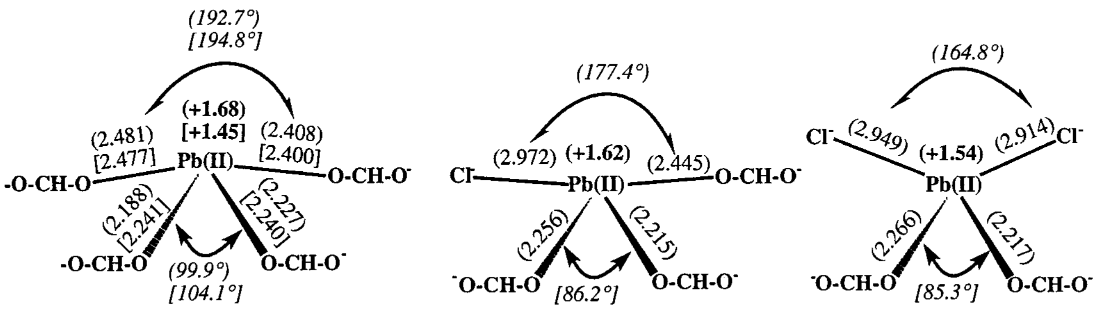

natural electron configuration	Pb:6s(1.84)6p(0.48);sp$^{0.26}$ Pb:6s[1.91]6p[1.45]6d[0.03];sp $^{0.76}$	Pb:6s(1.88)6p(0.49);sp$^{0.26}$	Pb:6s(1.90)6p(0.54);sp$^{0.28}$
lone pair NBO	Pb: s [92.60%] p 0.08 [7.39%]		
lone pair occupancy	[1.959]		
% NBO on Pb(II) (short bonds)			

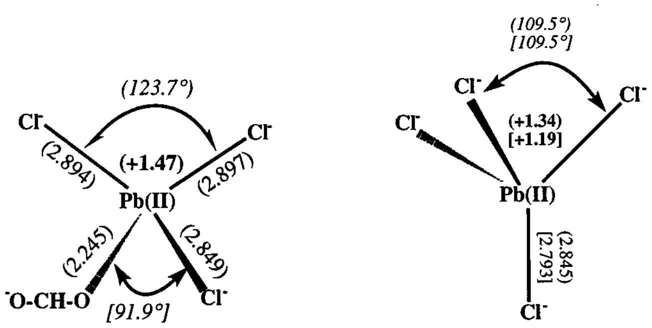

natural electron configuration	Pb:6s(1.96)6p(0.55);sp$^{0.28}$	Pb:6s(2.00)6p(0.63);sp$^{0.32}$ Pb:6s[1.96]6p[0.78]6d[0.02];sp$^{0.40}$
lone pair NBO		Pb: s [100%]
lone pair occupancy		[1.964]
% NBO on Pb(II)		5.2%

Figure 8. Geometries from ab initio molecular orbital calculations of Pb^{II}[HCO$_2^-$]$_n$[Cl]$_{4-n}$ when n = 0−4: ( ) MP2/LANL2DZ optimization; [ ] MP2/LANL2DZ+*d* optimization.

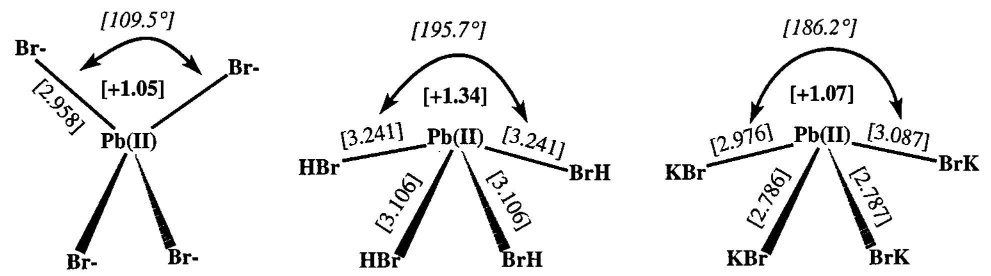

natural electron configuration	Pb:6s[1.96]6p[0.92]6d[0.02];sp$^{0.47}$	Pb:6s[1.96]6p[0.66]6d[0.02];sp$^{0.34}$	Pb:6s[1.91]6p[0.95]6d[0.02];sp$^{0.50}$
lone pair NBO	Pb: s [100%]	Pb: s [99.50%] p 0.00 [0.50%]	Pb: s [96.77%] p 0.03 [3.23%]
lone pair occupancy	[1.963]	[1.966]	[1.961]
short bonds, %Pb orbital	6.7%	8.0%	11.9%

Figure 9. Geometries from ab initio molecular orbital calculations of (a) Pb^{II}•4Br$^-$, (b) Pb^{II}•4BrH, and (c) Pb^{II}•4BrK: [ ] = MP2/LANL2DZ+*d* optimization.

Table 6. Factors Favoring Hemidirected or Holodirected Ligand Geometries

hemidirected (void in ligands)	holodirected (no void in ligands)
•lower coordination number	• higher coordination number
•hard ligands	• soft ligands
•attractive interactions among ligands	• repulsive interactions among ligands
•lone pair has p character	• lone pair has no p character
•fewer electrons transferred [from ligands to Pb(II)]	• more electron transferred [from ligands to Pb(II)]
•bonds more ionic	• bonds more covalent

the identity of liganding atom, interactions among the ligands, etc. A list of factors that tend to favor (but not rigorously determine) hemi- or holodirected arrangements of ligands is given in Table 6.

Knowledge of the factors that affect the coordination geometry of Pb(II) may be helpful in the design of complexing agents that can remove divalent lead and differentiate it from other harmless metal ions such as zinc and magnesium. It is possible to design ligands that will ensure a hemidirected environment of the Pb(II), but in that case there is a variation in the types of bonds to the lead as a function of their positional relationship with respect to the lone pair of electrons. On the other hand, if the arrangement is holodirected, the Pb^{II}−ligand bonds are all similar and are longer than those found in hemidirected geometries.[6] The chemist has a choice to make between these two possibilities.

Acknowledgment. We thank Drs. P. Pyykkö, G. Desiraju, E. Jaffe, and G. D. Markham for helpful discussions. We also thank Mr. G. P. Shields of the Department of Chemistry, University of Cambridge, Lensfield Road, Cambridge CB2 1EW, U.K., who checked the oxidation states of some of the CSD entries for us. We thank the Advanced Scientific Computing Laboratory, NCI-FCRF, for providing time on the CRAY YMP supercomputer. This work was supported by Grants CA-10925 and CA-06927 from the National Institutes of Health and by an appropriation from the Commonwealth of Pennsylvania. Its contents are solely the responsibility of the authors and do not necessarily represent the official views of the National Cancer Institute. This work is part of the dissertation of Liat Shimoni-Livny for the Ph.D. degree at the University of Pennsylvania.

Supporting Information Available: Listing of CSD reference codes and bibliographical information on the crystal structures used in this study and the crystal structures of the lead compounds that are not included (Table 1S); examples of *.que and *.geo files (Tables 2S and 3S, respectively), a list of *x*, *y*, and *z* coordinates of the optimized complexes from the ab initio molecular orbital calculations (Table 4S), and structures of $Pb^{II}\cdot 4OH^-$, $Pb^{II}\cdot OCHO^-$, $Pb^{II}\cdot 4Br^-$, $Pb^{II}\cdot 4BrH$, and $Pb^{II}\cdot 4BrK$ (24 pages). Ordering information is given on any current masthead page.

IC970909R